

Supporting Information

Adjusting CO₂ hydrogenation pathway via synergic effects of iron carbide and iron
oxide

Fangxu Lu, Xin Chen, Wen Wang*, Yi Zhang*

College of Chemical Engineering, Beijing University of Chemical Technology, 15 Beisanhuan East
Road, Beijing 100029, PR China

Corresponding Author

* Tel&Fax: +86 10 64436991

Email: wangwen@mail.buct.edu.cn (W.W.); yizhang@mail.buct.edu.cn (Y. Z.)

Experimental Section

Materials

Ferric chloride hexahydrate ($\text{FeCl}_3 \cdot 6\text{H}_2\text{O}$), trisodium citrate pentahydrate ($\text{Na}_3\text{C}_6\text{H}_5\text{O}_7 \cdot 5\text{H}_2\text{O}$), tritonX-100, sodium acetate was supplied by Tianjing Chemical Corp. Ethanol, ethylene glycol, and diethylene glycol were purchased from Beijing Chemical Corp. All chemicals are analytical reagent grade and used correctly in accordance with regulations. The water involved in the all experiments was deionized water.

Preparation of Fe_3O_4 microspheres

The Fe_3O_4 microspheres were synthesized via a solvothermal reaction approach. The premixed mixture $\text{FeCl}_3 \cdot 6\text{H}_2\text{O}$ (2.0 g) and tritonX-100 (0.2 g) was dissolved in ethylene glycol (40 mL) in a round bottomed flask (250 mL capacity) via magnetic stirrer. A solution of diethylene glycol (40 mL), which contain sodium acetate (4.0 g), was then added with magnetic stirring. Afterward, the mixture was stirred vigorously for 30 min. The obtained yellow solution was then transferred and sealed into a Teflon-lined stainless-steel autoclave with a capacity of 100 mL. The autoclave was heated at 200 °C and maintained for 10 h, and then cooled to room temperature. The products were repeatedly washed with ethanol and deionized water, respectively. The fresh Fe_3O_4 microspheres were obtained after dried at 60°C for 10 h in a vacuum.

Preparation of Na-promoted Fe_3O_4 microsphere catalysts

The Na-promoted Fe_3O_4 microsphere catalysts in the present work were prepared by the wet impregnation method. Briefly, the Na promoter loading of 2wt % was calculated amount from the precursor trisodium citrate pentahydrate ($\text{Na}_3\text{C}_6\text{H}_5\text{O}_7 \cdot 5\text{H}_2\text{O}$). After that, the obtained fresh Fe_3O_4 microspheres were modified via impregnating with an aqueous solution containing amount of

trisodium citrate pentahydrate ($\text{Na}_3\text{C}_6\text{H}_5\text{O}_7 \cdot 5\text{H}_2\text{O}$), which were denoted as Na/ Fe_3O_4 . Then the Na-promoted Fe_3O_4 microsphere samples were allowed by drying at 120 °C under vacuum. All obtained powder samples were reconstructed into pellets (10 MPa), crushed and selected 20-40 mesh particles for CO_2 hydrogenation reaction tests.

Catalyst characterization

Powder X-ray diffraction (XRD) measurements of the fresh and spent catalysts were analyzed in the 2θ range from 20 to 80° on X-ray diffractometer (SHIMADZU XRD-6000) with $\text{Cu K}\alpha$ radiation ($\lambda=0.154$ nm), operating at 40 kV and 30 mA at a scanning rate of 5° min^{-1} . The scan mode is continuous scan and the sampling pitch is 0.02°. The crystallite phase of all samples was determined by standard XRD pattern of the International Diffraction Data Center.

The specific surface area and total pore volume of the catalysts were determined by N_2 adsorption-desorption measurements at -196 °C, using an automated surface area and pore size analyzer (Micrometrics ASAP 2020 equipment). Before the adsorption measurements, the sample was degassed at 180 °C for 6 h under vacuum.

CO_2 temperature-programmed desorption (CO_2 -TPD) was carried out on Quantachrome automated gas sorption analyzer. About 0.1 g amount of sample was pretreated at 200 °C for 1 h under N_2 to remove possible impurities. CO_2 adsorption was carried out at room temperature for 30 min at a stream of 5 vol% CO_2 -95vol% Ar. Before the TPD experiments, the physically adsorbed CO_2 was removed by Ar for 2 h. After pretreatment, the temperature was increased to 800 °C with a temperature rate of 5 °C· min^{-1} in the flow of Ar gas, and the desorbed CO_2 was continuously monitored by a TCD detector.

The X-ray photoelectron spectroscopy (XPS) measurements were manufactured by SHIMADZU AXIS Supra X-ray photoelectron spectrometer equipped with an Al K α radiation. Prior to experiment, the spent catalysts kept at the glove box were prepared under the Ar atmosphere, and the samples were transferred to the reaction chamber, strictly avoiding air during the whole process. Next, in-situ pretreated with a high purity Ar stream at 200°C for 2h to remove the residual hydrocarbon on the catalyst surface. After pretreated, the samples were then cooled to room temperature and transferred to the analysis chamber without exposure to air for obtaining the XPS data. All the binding energies were calibrated by the C1s peak at 284.8 eV.

The size, morphology and element distribution were analyzed by scanning electron microscope (SEM, Zeiss Supra55). The further insights into the surface morphology and structure were acquired on the high-resolution transmission electron microscope (HR-TEM, JEOL, JEM-2100F). High angle annular dark-field scanning transmission electron microscopy (HAADF-STEM), and energy dispersive X-ray spectroscopy (EDX), were performed on a FEI Tecnai G2 F20 S-Twin transmission electron microscope equipped with an EDX detector. All the specimens were prepared by ultrasonically suspending the sample in ethanol. Afterward, a drop of the suspension was deposited on a coverslip or Ultra-thin carbon film grids and dried in air.

Hydrogen temperature-programmed reduction (H₂-TPR) experiments were performed on a FINESORB-3010 temperature programmed reduction device, which equipped with a thermal conductivity detector (TCD) to detect the H₂ contents of the tail gas. H₂-TPR experiments were carried out in a quartz tube reactor using 50 mg prepared catalysts. Before the experiments, the sample was in-situ pretreated with a high purity Ar stream (30 mL·min⁻¹) at 120 °C to remove the

residual water. After pretreatment, the temperature was increased to 800 °C with a temperature rate of 10 °C·min⁻¹ in the flow of a 10% H₂/90% Ar gas mixture (30 mL·min⁻¹).

Near ambient pressure X-ray photoelectron spectroscopy (NAP-XPS) experiments of spent catalysts were performed in a SPECS system with base pressure of 5×10^{-10} mbar. Prior to NAP-XPS characterization, the spent catalysts were reduced by the syngas (H₂/CO=1, 30 mL·min⁻¹) for 2 h at 300 °C, followed by cooling down to 30 °C at Ar stream. After preparation, the catalyst was moved to the XPS analyzer, and a total of 400 mtorr gases (100 mtorr CO₂ and 300 mtorr H₂) were dosed into the main chamber at 30 °C. After gas exposure, the catalyst was heated up to 300 °C for reaction, and the surface carbon species were recorded by NAP-XPS at 30°C, 150°C and 300 °C. All XPS spectra were acquired using a monochromatic Al K α X-ray source ($h\nu = 1486.6$ eV). The spectrometer was calibrated using the Au 4f_{7/2} peak of a clean Au (111) sample before experiments.

Mössbauer spectroscopy measurements were conducted at room temperature in an MR-351 constant-acceleration Mossbauer spectrometer (FAST, Germany), using a 25 mCi ⁵⁷Co in Pd matrix. Data analysis was performed using a nonlinear least-squares fitting routine that modeled the spectra as a combination of singlets, quadruple doublets, and magnetic sextets based on a Lorentzian lineshape profile. The components were identified based on their isomer shift (IS), quadruple splitting (QS), and magnetic hyperfine fields (Hhf). Magnetic hyperfine fields were calibrated with the 330 kOe field of α -Fe foil.

The in-situ diffuse reflectance infrared Fourier transform spectra (in-situ DRIFTS) experiments were recorded with a Bruker Tensor 27 spectrometer, which equipped with a liquid nitrogen-cooled MCT detector, using a diffuse reflectance infrared cell with ZnSe windows. To get clear spectra, the spent catalysts were diluted by KBr. Before in-situ DRIFTS characterization, the diluted samples

(about 15 mg) were exposed to high purity Ar ($30 \text{ mL}\cdot\text{min}^{-1}$) gas flow at $200 \text{ }^\circ\text{C}$ for 1 h to remove the residual water and other contamination. Afterward, CO_2 was introduced into the cell for 0.5 h, and then the H_2 (5% H_2 /95% Ar, $30 \text{ mL}\cdot\text{min}^{-1}$) was introduced to the sample, and the H_2 adsorption began. The background spectrum of the sample was collected before CO_2 adsorption. All the above experiments were conducted at ambient pressure and $200 \text{ }^\circ\text{C}$. All the spectra were recorded at a resolution of 4 cm^{-1} and accumulation of 32 scans.

Catalytic reaction

CO_2 hydrogenation reactions were conducted in a stainless fixed-bed reactor (inner diameter 8 mm). For all the experiments, catalyst (20-40 mesh, 0.5 g) diluted with quartz granule (20-40 mesh, 1 g) was loaded into the fixed-bed reactor. The flow rates of the gases were controlled using mass flow meters (5850E, Brooks). The mixture gas flow composition was, 71.25% H_2 : 23.75% CO_2 : 5% Ar (volume ratio), unless otherwise indicated, where Ar was used as inner reference gas. The reactor was raised to $300 \text{ }^\circ\text{C}$ at a heating rate of $2^\circ\text{C}/\text{min}$ at 0.1 MPa by syngas ($\text{H}_2/\text{CO}=1$), and then the reduction progress was carried out in-situ for 10 hours by syngas, followed by cooling down to $80 \text{ }^\circ\text{C}$ in N_2 . After that, the pressure of the reactor was regulated to 0.5 or 3 MPa by the mixture gas, the temperature of reactor was ramped to $300 \text{ }^\circ\text{C}$ at a heating rate of $10^\circ\text{C}/\text{min}$. Afterward, the CO_2 hydrogenation reaction was continuously carried out at $300 \text{ }^\circ\text{C}$, 0.5 MPa /3.0 MPa, $\text{H}_2/\text{CO}_2=3$, and GHSV= $2500 \text{ mL}/\text{g}\cdot\text{cat}\cdot\text{h}^{-1}$ for 50 hours. The spent catalysts, tested under different reaction pressure, were respectively denoted as Fe_3O_4 0.5 MPa, Fe_3O_4 3.0 MPa, Na/ Fe_3O_4 0.5 MPa, Na/ Fe_3O_4 3.0 MPa. After reaction, the sample collection is done inside the glovebox by placing the reaction tube inside without any exposure to the air, and the collected spent catalysts were kept in an Ar-filled glovebox to avoid overoxidation before further characterization.

The effluent gas from the reactor was analyzed by on-line gas chromatography (GC-2014C, Shimadzu). The Ar, CO, and CO₂ contents of the outlet gases were determined by using a activate carbon column with a thermal conductivity detector (TCD), using H₂ as the carrier gas. Hydrocarbons (C₁–C₅) were analyzed on-line using Porapak-Q column with an N₂ carrier and a hydrogen flame ionization detector (FID). The collected liquid products (C₅₊) and oxygenates were analyzed offline on GC-FID with an N₂ carrier by silicone SE-30 column and Plot Q capillary column, respectively. The calculated mass balance is almost 95%, which is based on the moles of carbon in all reactions.

The CO₂ conversion was calculated based on the following Eq:

$$CO_2 \text{ Conversion} = \frac{\frac{CO_{2in}}{Ar} - \frac{CO_{2out}}{Ar}}{\frac{CO_{2in}}{Ar}}$$

The carbon balance of produce was given according to the following Eq:

$$\text{Carbon balance} = \frac{\text{The mol of CO} + \sum_{i=1}^n \text{mol of } C_i \text{ product}}{\text{The toatl mol of CO}_2} \times 100\%$$

Where C_i is the product i (hydrocarbon or oxygenates),

The selectivity of individual hydrocarbon or oxygenates product S_i was calculated from the following Eq:

$$S_i = \frac{M_i \times X_i}{\sum_{i=1}^n M_i \times X_i} \times 100\%$$

Where M_i is the relative molecular mass of product i (hydrocarbon or oxygenates), X_i is the mole fraction of product i (hydrocarbon or oxygenates).

The Yield of alkenes produce was given according to the following Eq:

$$Yield = CO_{2_{Conversion}} \times (1 - CO_{selectivity}) \times CH_{n_{selectivity}} \times Alkenes_{selectivity\ in\ CHn} \times 100\%$$

The Yield of ethanol produce was given according to the following Eq:

$$Yield = CO_{2_{Conversion}} \times (1 - CO_{selectivity}) \times ROH_{selectivity} \times Ethanol_{selectivity\ in\ ROH} \times 100\%$$

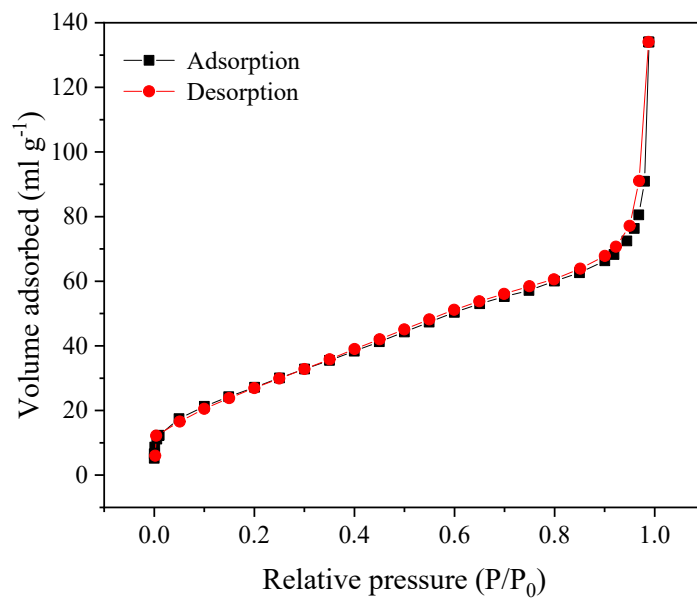


Figure S1. N₂ adsorption-desorption isotherms of the fresh Fe₃O₄ microsphere catalyst.

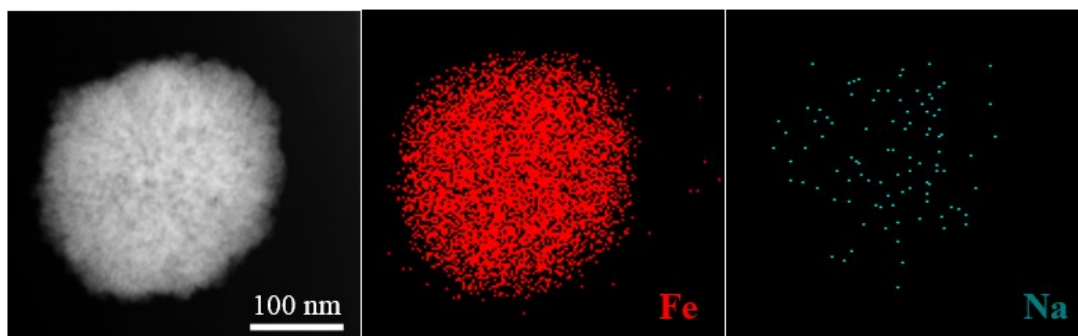


Figure S2. STEM-EDX elemental mapping of fresh Na/Fe₃O₄ catalyst.

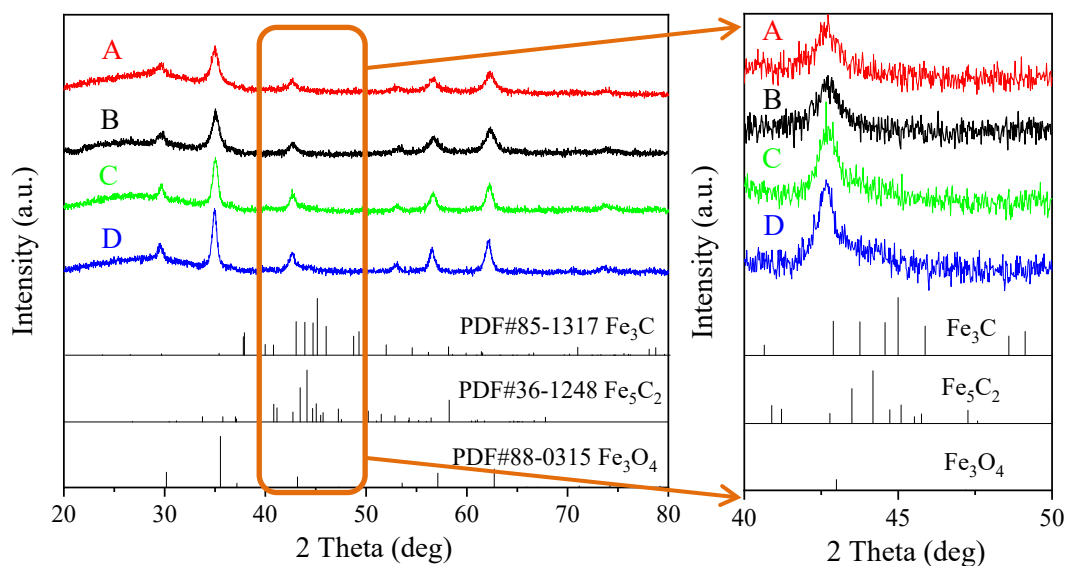


Figure S3. XRD patterns for the spent catalysts 0.5 MPa reaction: A) Na/Fe₃O₄ catalyst and B) Fe₃O₄ catalyst; 3.0 MPa reaction: C) Na/Fe₃O₄ catalyst and D) Fe₃O₄ catalyst.

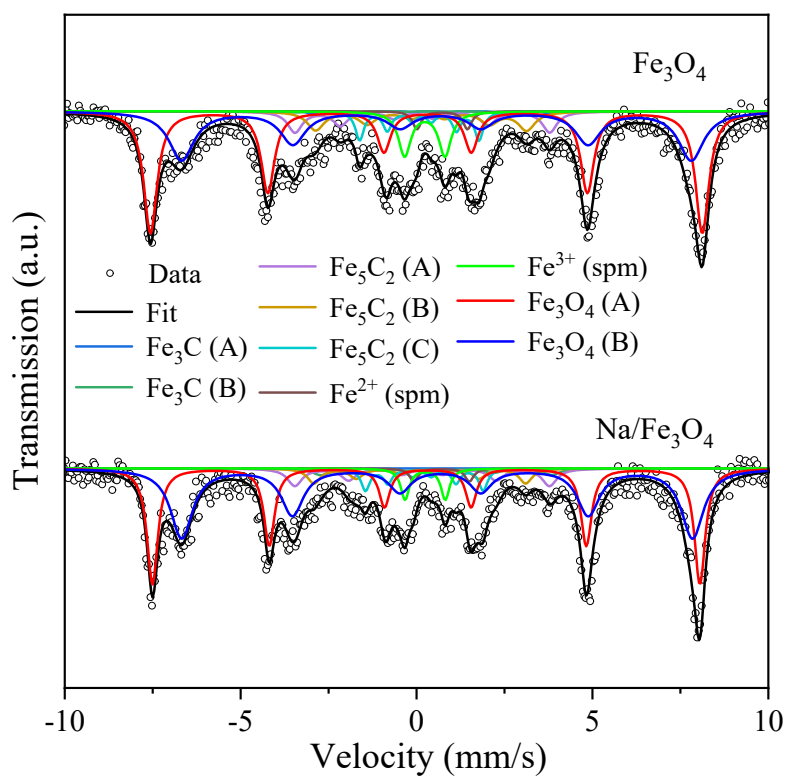


Figure S4. Mössbauer spectroscopy of various reduced catalysts.

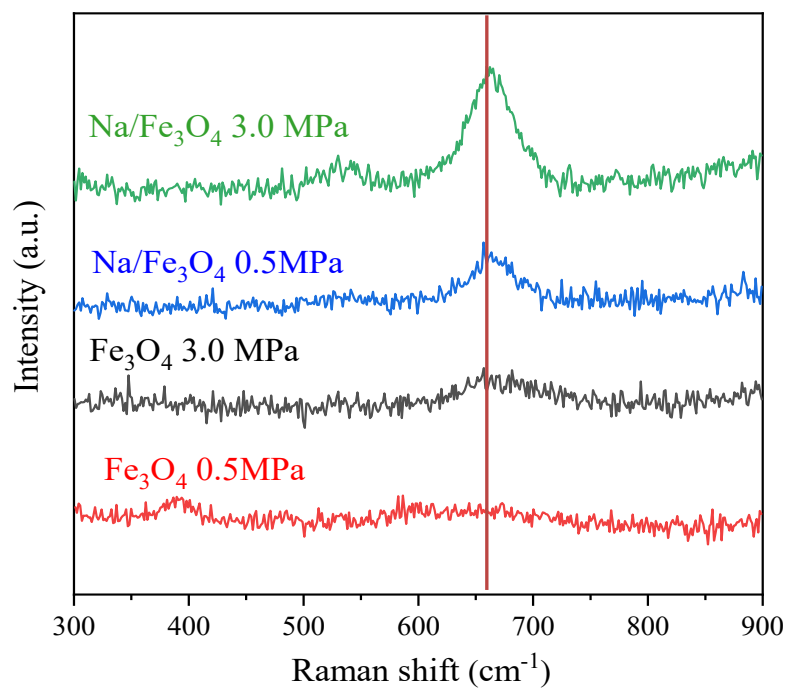


Figure S5. Raman spectra of the of various reduced catalysts.

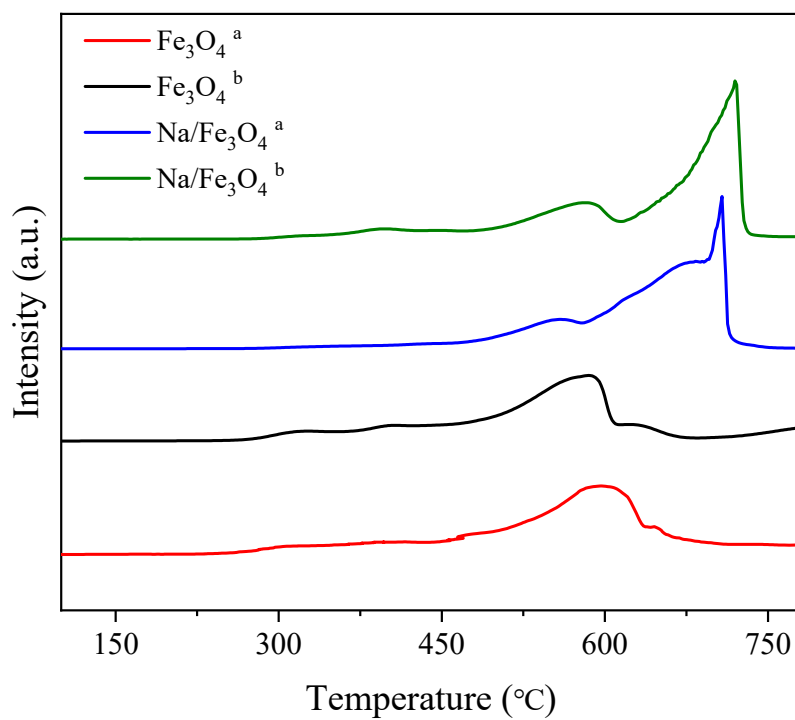


Figure S6. The CO_2 -TPD of various spent catalysts. a) 0.5 MPa reaction; b) 3.0 MPa reaction.

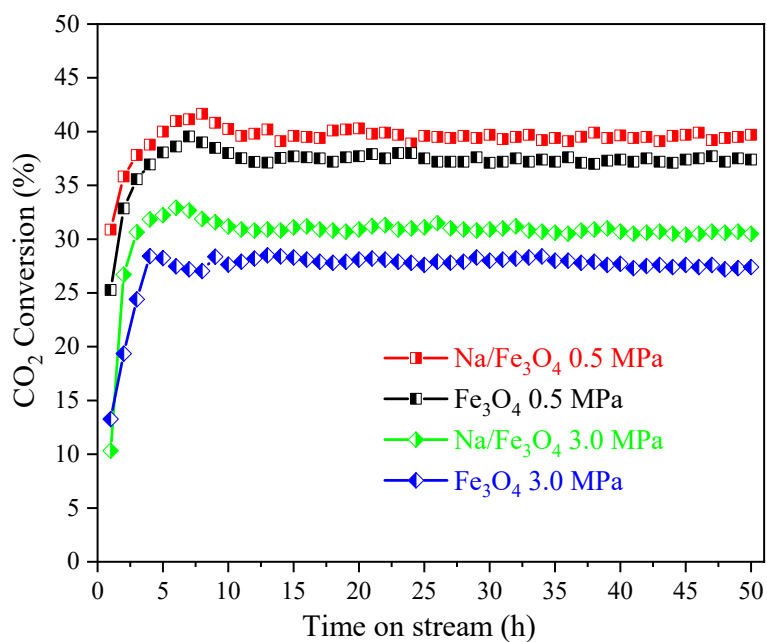


Figure S7. CO₂ conversion and stability test of the catalysts. Reaction conditions: 300 °C, 0.5 MPa /3.0 MPa, H₂/CO₂=3, and GHSV=2500 mL/g-cat·h⁻¹ for 50 hours.

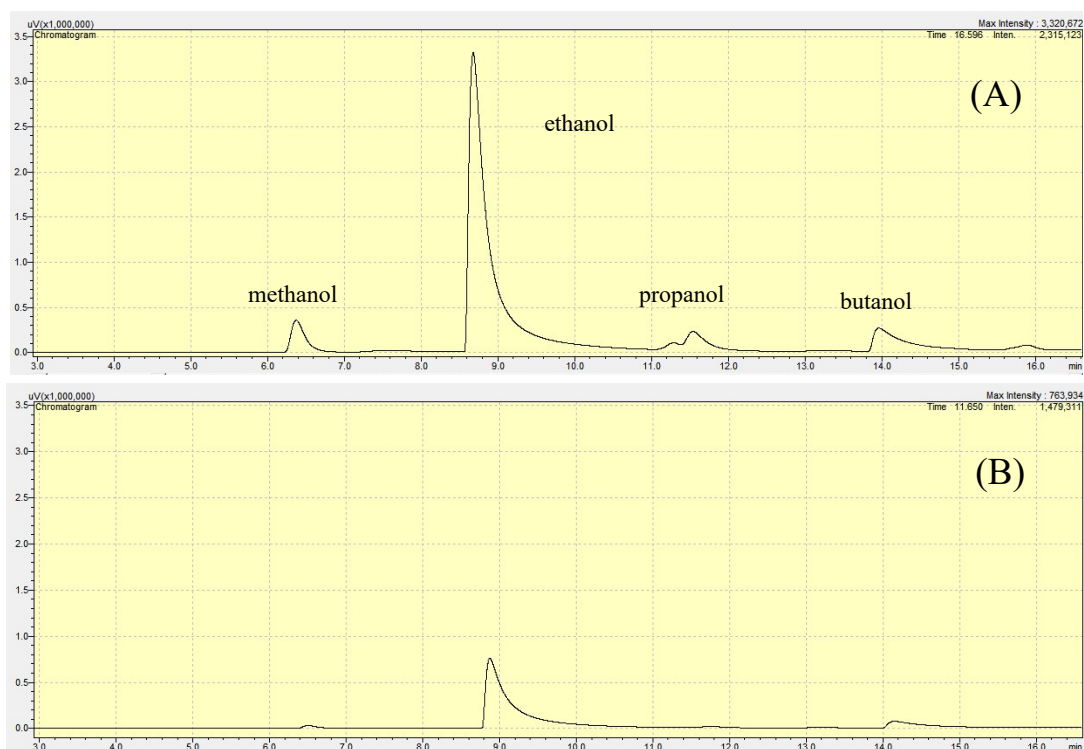
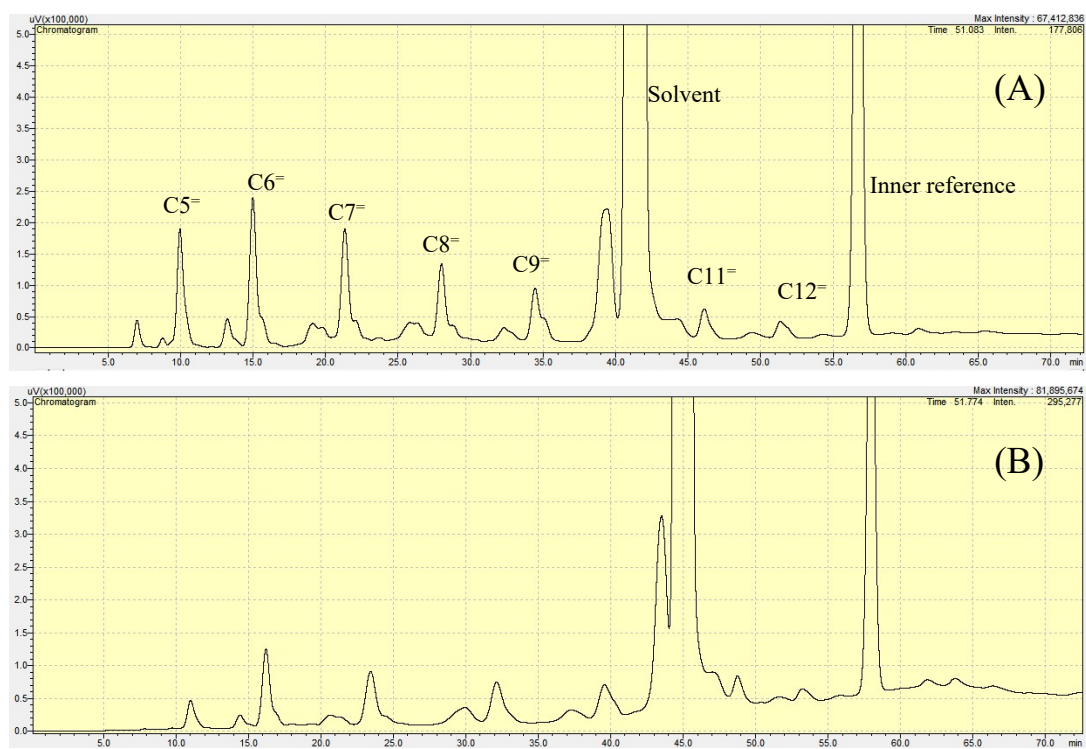


Figure S8. GC spectra of liquid phases (alcohol phase) of the iron-based catalysts: (A) Na/Fe₃O₄

3.0MPa, (B) Na/Fe₃O₄ 0.5MPa.



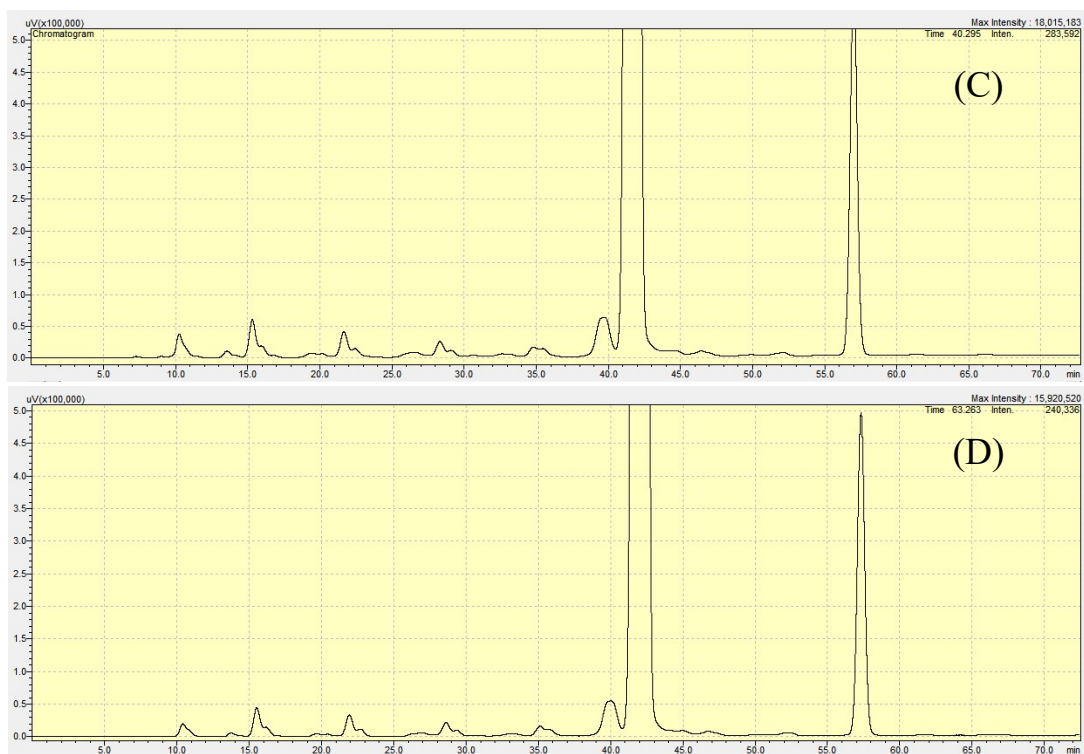
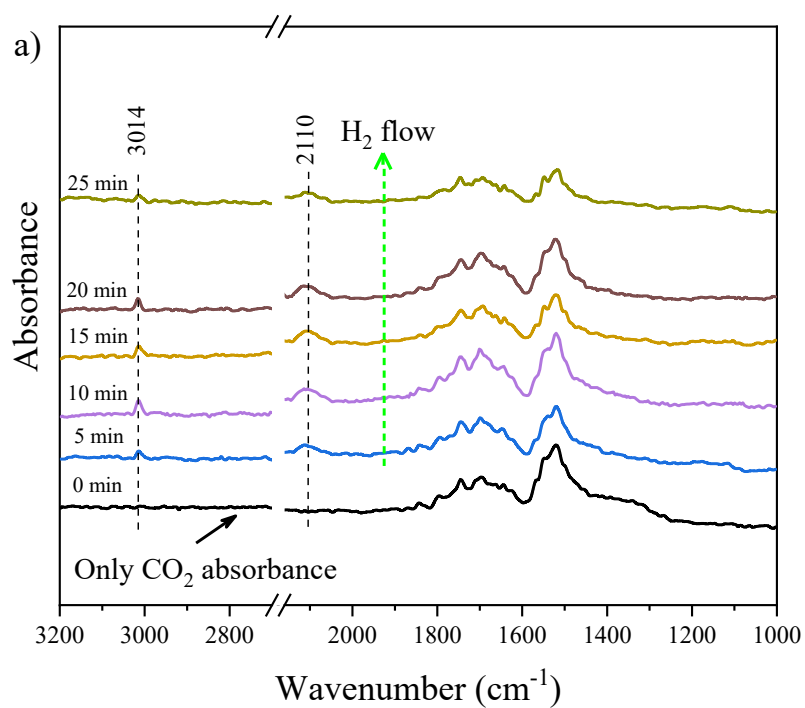


Figure S9. GC spectra of liquid phases (liquid phases) of the iron-based catalysts: (A) Na/Fe₃O₄ 0.5 MPa, (B) Na/Fe₃O₄ 3.0 MPa, (C) Fe₃O₄ 0.5 MPa, (B) Fe₃O₄ 3.0 MPa.



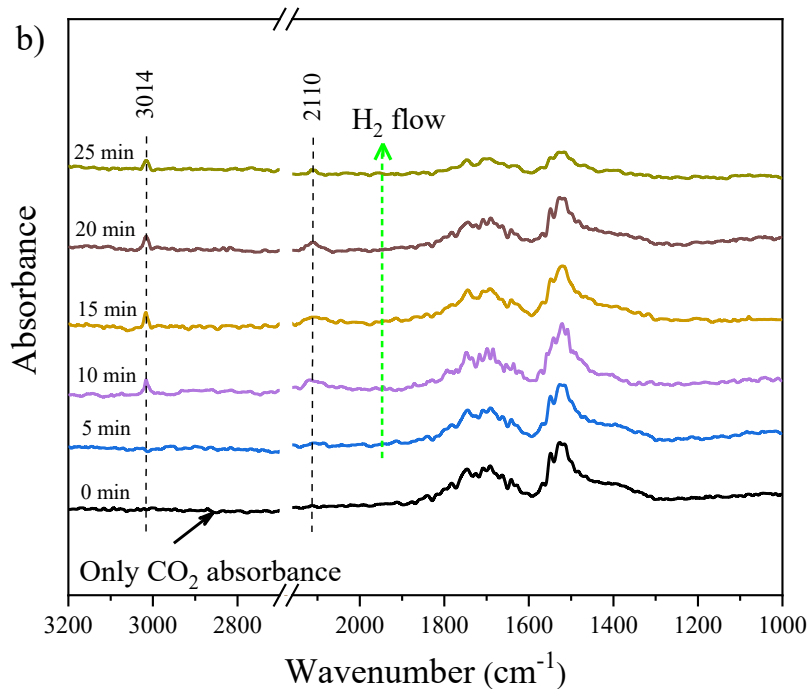


Figure S10. In-situ CO₂-DRIFT spectra of the spent un-promoted Fe₃O₄ catalysts. a) 0.5 MPa reaction and b) 3.0 MPa reaction.

Table S1. Mössbauer parameters of the reduced catalysts.

Catalysts	Phases	Mössbauer parameters			
		IS (mm/s)	QS (mm/s)	Hhf (kOe)	Area (%)
Fe ₃ O ₄	Fe ₅ C ₂	0.05	0.23	225	7.4
		0.23	-0.20	186	7.7
		0.11	-0.07	105	5.9
	Fe ₃ C	0.39	-0.003	210	0.5
		0.05	-0.30	207	0.5
	Fe ₃ O ₄ (A)	0.30	-0.04	487	39.7
	Fe ₃ O ₄ (B)	0.62	-0.12	450	29.7
	Fe ²⁺ (spm)	0.73	1.43		1.9
Fe ³⁺ (spm)	0.24	1.15		6.7	
Na/Fe ₃ O ₄	Fe ₅ C ₂	0.15	-0.006	225	7.8
		0.05	0.06	187	6.2

		0.17	0.07	104	6.0
	Fe ₃ C	0.40	0.30	204	2.9
	Fe ₃ O ₄ (A)	0.28	-0.05	483	31.6
	Fe ₃ O ₄ (B)	0.62	-0.09	451	40.4
	Fe ²⁺ (spm)	0.70	1.57		1.5
	Fe ³⁺ (spm)	0.23	1.14		3.6

Table S2. The results of in-situ XPS for Fe 2p_{3/2}.

Catalysts	Binding energy (eV)				Surface content of iron species				Fe ²⁺ /Fe ³⁺
	Fe 2p _{3/2}				(atom%) Fe 2p _{3/2}				
	Fe ₅ C ₂	Fe ₃ C	Fe ²⁺	Fe ³⁺	Fe ₅ C ₂	Fe ₃ C	Fe ²⁺	Fe ³⁺	
Fe ₃ O ₄ ^a	707.2	708.3	709.7	711.7	28.7	7.1	31.4	32.8	0.95
Na/Fe ₃ O ₄ ^a	707.1	708.0	709.6	711.6	25.1	17.6	35.4	21.8	1.62
Fe ₃ O ₄ ^b	707.2	708.2	709.8	711.8	16.1	4.9	36.8	42.1	0.87
Na/Fe ₃ O ₄ ^b	707.0	708.1	709.6	711.6	24.0	10.8	48.1	17.0	2.83

^a CO₂-0.5 MPa reaction.

^b CO₂-3.0 MPa reaction.

Table S3. The results of in-situ XPS for O 1s.

Catalysts	Binding energy (eV)			Surface content of O species		
	O 1s			(atom%)		
	Fe ₃ O ₄	O _{lattice}	O _{defect}	Fe ₃ O ₄	O _{lattice}	O _{defect}
Fe ₃ O ₄ ^a	529.7	531.5	533.1	39.1	45.9	15.0
Na/Fe ₃ O ₄ ^a	529.8	531.9	533.5	23.1	48.1	28.8
Fe ₃ O ₄ ^b	529.7	531.4	533.4	26.8	56.4	16.8
Na/Fe ₃ O ₄ ^b	529.8	532.0	533.4	27.3	39.6	33.1

^a CO₂-0.5 MPa reaction.

^b CO₂-3.0 MPa reaction.

Table S4. Comparison of the catalytic performance for the formation of alkenes from CO₂ hydrogenation in literatures.

Catalysts	CO ₂ conv.%	CO Sel. %	Hydrocarbon sel. (wt%)			alkenes Yield %	Ref.
			CH ₄	alkenes	others		
In ₂ O ₃ -ZrO ₂ /SAPO-34	35.5	85.0	4.3	76.4 ^a	19.3	4.1	1
Zn-ZrO ₂ /ZnSAPO-34	12.6	47.0	3.0	80.0 ^a	17.0	5.3	2
ZnGa ₂ O ₄ /SAPO-34	13.0	49.0	1.0	86.0 ^a	13.0	5.7	3
Fe ₂ N@C	33.7	15.8	46.0	31.0	23.0	8.8	4
Fe/C-bio	30.5	23.2	11.8	72.0	16.2	16.9	5
Fe ₂ O ₃ @KO ₂	48.3	15.9	15.2	57.4	27.4	23.3	6
Na/Fe ₃ O ₄ 0.5 MPa	39.6	7.1	18.0	73.2	8.8	22.03	This work

^a C₂=C₄=olefins.

Note: Alkenes yield max error $\leq \pm 1\%$.

Table S5. Comparison of the catalytic performance for the formation of ethanol from CO₂ hydrogenation in literatures.

Catalysts	CO ₂ conv.%	CO Sel. %	Product sel. (wt%)			ethanol Yield %	Ref.
			CH _n	ROH	Ethanol (in ROH)		
Na-Co/SiO ₂	18.8	29.1	86.6	13.4	62.8	1.12	7
RhFeLi/TiO ₂ NRs	15.7	12.5	36.3	63.7	95.3	8.33	8
Rh-0.3VO _x / MCM-41	12.1	20.1	36.4	63.6	82.2	5.04	9
Mesoporous- Co ₃ O ₄	12.5	-	36.1	63.9	48.2	3.85	10
Cu@Na-Beta	7.9	30.5	-	100	100	5.49	11
Na/Fe ₃ O ₄ 3.0 MPa	30.6	4.1	56.2	43.8	87.4	11.23	This work

Note: ethanol yield max error $\leq \pm 1\%$.

Table S6. The activity and selectivity of various pressure for the Na/Fe₃O₄ catalyst.

Catal.	CO ₂ conv. (%)	CO ₂ to CO (%)	Product		Hydrocarbon Selectivity in CH _n				Alcohol Selectivity in		
			Selectivity		(wt %)				ROH (wt %)		
			CH _n	ROH	CH ₄	Alkenes (C ₂₊)	Alkanes (C ₂₊)	O/P ^c	MeOH	EtOH	C ₂₊ OH
0.25 MPa	30.6	15.5	99.5	0.5	37.5	47.8	14.7	6.0	-	-	-
1.0 MPa	40.2	6.2	80.2	19.8	19.1	68.8	12.1	9.6	5.1	65.7	29.2
2.0 MPa	37.0	5.9	78.5	21.5	21.5	63.3	15.2	8.1	4.5	75.2	20.3
4.0 MPa	29.5	5.1	68.1	31.9	27.1	56.0	16.9	4.1	3.8	79.7	16.5

Reaction conditions: 300°C, H₂/CO₂ = 3, GHSV=2500 mL/g-cat·h⁻¹.

References

1. P. Gao, S.S. Dang, S.G. Li, X. Bu, Z.Y. Liu, M.H. Qiu, C.G. Yang, H. Wang, L.S. Zhong, Han, Y., Q. Liu, W. Wei, and Y. Sun, *ACS Catal.*, 2018, **8**, 571-578.
2. Z. Li, J. Wang, Y. Qu, H. Liu, C. Tang, S. Miao, Z. Feng, H. An, and C. Li, *ACS Catal.*, 2017, **7**, 8544-8548.
3. X. Liu, M. Wang, C. Zhou, W. Zhou, K. Cheng, J. Kang, Q. Zhang, W. Deng, and Y. Wang, *Chem. Commun.*, 2018, **54**, 140-143.
4. B. Zhao, M. Sun, F. Chen, Y. Shi, Y. Yu, X. Li, and B. Zhang, *Angew. Chem. Int. Ed.*, 2021, **60**, 1-6.
5. L. Guo, J. Sun, X. Ji, J. Wei, Z. Wen, R. Yao, H. Xu, and Q. Ge, *Commun. Chem.*, 2018, **1**, 11.
6. A. Ramirez, A.D. Chowdhury, A. Dokania, P. Cnudde, M. Caglan, I. Yarulina, E. Abou-Hamad, L. Gevers, S. Ould-Chikh, K. De Wispelaere, V. van Speybroeck, and J. Gascon, *ACS Catal.*, 2019, **9**, 6320-6334.
7. S. Zhang, X.F. Liu, Z.L. Shao, H. Wang, and Y.H. Sun, *J. Catal.*, 2020, **382**, 86-96.
8. C.S. Yang, R.T. Mu, G.S. Wang, J. Song, H. Tian, Z.-J. Zhao, and J.L. Gong, *Chem. Sci.*, 2019, **10**, 3161-3167.
9. G. Wang, R. Luo, C. Yang, J. Song, C. Xiong, H. Tian, Z.J. Zhao, R. Mu, and J. Gong, *Sci. China*

-
- Chem., 2019, **62**, 1710-1719.
10. B. Liu, B. Ouyang, Y. Zhang, K. Lv, Q. Li, Y. Ding, and J. Li, *J. Catal.*, 2018, **366**, 91-97.
 11. L.P. Ding, T. Shi, J. Gu, Y. Cui, Z.Y. Zhang, C.J. Yang, T. Chen, M. Lin, P. Wang, N.H. Xue, L. Peng, X. Guo, Y. Zhu, Z. Chen, and W. Ding, *Chem*, 2020, **6**, 1-17.